CONF-750804--10

TRANSIENT PROPAGATION BEHAVIOR OF TWO-PHASE FLOW EQUATIONS

by

Robert W. Lyczkowski

TRANSIENT PROPAGATION BEHAVIOR OF TWO-PHASE FLOW EQUATIONS

BY

Robert W. Lyczkowski

Aerojet Nuclear Company*
550 Second St.
Idaho Falls, Idaho 83401

A paper submitted to the Session, "Two Phase Flow", Dimitri Gidaspow, Chairman at the 15th National Heat Transfer Conference, San Francisco, August 10 - 13, 1975

* Work performed for the U. S. Nuclear Regulatory Commission.

TRANSIENT PROPAGATION BEHAVIOR OF TWO-PHASE FLOW EQUATIONS

BY

Robert W. Lyczkowski

ABSTRACT

The capability of published two-phase flow equation sets to predict transient propagation behavior has been studied numerically. The equation sets are those cited by Wallis[1] for separated flow and extensions of those used by Rudinger and Chang[2] for dispersed flow. The primary difference between these two sets is that in the set cited by Wallis, the pressure gradient appearing in each momentum equation is weighted by the phase volume fraction, whereas in the extended Rudinger-Chang set, the pressure gradient appears only in the "continuous" phase. The original Rudinger-Chang set had to be modified because it can adequately describe only the transient flow of very dilute suspensions of solids in air.

This numerical study shows that pressure pulses propagate at essentially the sound speeds obtained from characteristics analysis for the equation sets investigated. Comparisons of numerical results with experimental air-water pressure propagation data[3] show that only the modified Rudinger-Chang equation set exhibits propagation behavior in good agreement with the experimental observations at low (less than 10 percent) void fractions. None of the equation sets adequately predict the experimental pressure propagation rates in the range of void fractions from 10 to 60 percent where the flow regime was observed to change from bubbly to full slug flow[3]. The modified Rudinger-Chang set explains an apparent discontinuity in the experimental pressure wave propagation speed at a void fraction of 50 percent if the entire pressure gradient is assumed to be carried by the liquid for less than 50 percent voids and by the vapor for greater than 50 percent voids; however, the magnitude of the calculated discontinuity is greater than the experimental discontinuity.

Acknowledgment

Thanks are expressed to C. W. Solbrig, G. A. Mortensen, R. E. Narum and C. Noble for developing the numerical schemes to solve the basic equations in this paper, to J. A. McFadden for developing the air-water properties subcodes, and to W. J. Wnek for writing the simplified steam properties subcodes.

Nomenclature

Roman

C_i = Sound speed of phase i, ft/sec

C_m = Homogeneous sound speed given by Equation 30, ft/sec

C_s = Stratified sound speed given by Equation 6, ft/sec

C = Solids heat capacity, Btu/ (lb_m-°R)

C_p, C_v = Gas heat capacity at constant pressure and constant volume, Btu/ (lb_m-°R)

P = Pressure, psia

S_i = Entropy of phase i, Btu/ (lb_m-°R)

T_i = Temperature of phase i, °R

t = Time, sec

U_i = Internal energy of phase i, Btu/lb_m

v^i = Velocity of phase i, ft/sec

x = Spatial dimension, ft

Greek

α^i = Volume fraction of phase i, dimensionless

λ = Characteristic velocity, ft/sec

ρ_i = Thermodynamic density of phase i, lb_m/cu ft

ρ^ℓ = Dense phase partial density, lb_m/cu ft

ρ_m = Mixture density given by Equation 31, lb_m/cu ft

Subscripts and Superscripts

c = Continuous phase

g = Gas phase

ℓ = Liquid phase

1. Introduction

In single phase (or homogeneous) flow, described by a single continuity and momentum equation, pressure pulses travel into a motionless medium along the characteristic given by the adiabatic sound speed. In two-phase flow, described by separate continuity, momentum and energy equations for each phase (Unequal Velocity, Unequal Temperature, UVUT), the correspondence between characteristics and pressure propagation is not so clear[4]. For example, the characteristics for the two-phase flow equation set

Continuity

$$\frac{\partial(\alpha^g \rho_g)}{\partial t} + \frac{\partial}{\partial x}(\alpha^g \rho_g v^g) = 0 \tag{1}$$

$$\frac{\partial(\alpha^\ell \rho_\ell)}{\partial t} + \frac{\partial}{\partial x}(\alpha^\ell \rho_\ell v^\ell) = 0 \tag{2}$$

Momentum

$$\frac{\partial(\alpha^g \rho_g v^g)}{\partial t} + \frac{\partial}{\partial x}(\alpha^g \rho_g v^g v^g) + \alpha^g \frac{\partial P}{\partial x} = 0 \tag{3}$$

$$\frac{\partial(\alpha^\ell \rho_\ell v^\ell)}{\partial t} + \frac{\partial}{\partial x}(\alpha^\ell \rho_\ell v^\ell v^\ell) + \alpha^\ell \frac{\partial P}{\partial x} = 0 \tag{4}$$

are complex valued for all nonzero relative velocities for incompressible phases[5] and for all nonzero subsonic relative velocities for compressible steam-water mixtures[6]. Equations 1 - 4 are the ones cited by Wallis[1] with his "left over" terms, f_i, body forces, and mass source terms equal to zero[a]. In the absence of phase interaction terms, the phases are coupled by the requirement that $\alpha^\ell + \alpha^g = 1$.

---

[a] According to Giot and Fritte,[7] Delhaye[8] derived the proper three dimensional conservation equations, and Vernier and Delhaye[9] showed how to obtain the mean values of these equations over a pipe cross section. In one dimension these equations reduce to Equations 1-4. Boure[10], working independently, also found the one dimensional equations to possess complex characteristics.

The characteristics are real for a two phase mixture when the phases flow at equal velocities, and are given by

$$\lambda = -\frac{dx}{dt} = -v \pm C_s \tag{5a}$$

and

$$\lambda = -v^{\ell} = -v^{g} = -v \tag{5b}$$

where C_s is the so-called stratified sound speed given by[1]

$$C_s = \left[\frac{\rho_g \alpha^{\ell} + \rho_{\ell} \alpha^{g}}{\alpha^{\ell} \rho_g C_{\ell}^{-2} + \alpha^{g} \rho_{\ell} C_g^{-2}} \right]^{\frac{1}{2}} \tag{6}$$

and C_{ℓ} and C_g are the appropriate single phase sound speeds.

The characteristics for the Rudinger-Chang[2] two phase equation set are real for all relative velocities and are given by

$$\lambda = -v^{\ell} \text{ (three times)} \tag{7a}$$

$$\lambda = -v^{g} \tag{7b}$$

$$\lambda = -v^{g} \pm C_g \tag{7c}$$

This paper generalizes the Rudinger-Chang equation set to nondilute suspensions. The pressure propagation behavior of this modified equation set and the set quoted by Wallis is studied numerically and compared with experimental data.

2. Characteristics Analysis of the Rudinger-Chang UVUT Equation Set

The characteristics analysis for the Rudinger-Chang UVUT equation set is performed in order to show clearly the assumptions which are made in order to arrive at the characteristics given by Equations 7a - 7c.

The basic equations of mass, momentum, and energy conservation for the case of zero friction and zero heat and mass transfer are:

Continuity

$$\frac{\partial \rho_g}{\partial t} + \frac{\partial (\rho_g v^g)}{\partial x} = 0 \tag{8}$$

$$\frac{\partial \rho^\ell}{\partial t} + \frac{\partial (\rho^\ell v^\ell)}{\partial x} = 0 \tag{9}$$

Momentum

$$\frac{\partial (\rho_g v^g)}{\partial t} + \frac{\partial (\rho_g v^g v^g)}{\partial x} + \frac{\partial P}{\partial x} = 0 \tag{10}$$

$$\frac{\partial (\rho^\ell v^\ell)}{\partial t} + \frac{\partial (\rho^\ell v^\ell v^\ell)}{\partial x} = 0 \tag{11}$$

Energy

$$\frac{\partial}{\partial t}\left[\rho_g\left(\frac{1}{2} v^g v^g\right) + C_v T_g + \rho^\ell\left(\frac{1}{2} v^\ell v^\ell + C T_\ell\right)\right]$$

$$+ \frac{\partial}{\partial x}\left[\rho_g v^g\left(\frac{1}{2} v^g v^g + C_p T_g\right) + \rho^\ell v^\ell\left(\frac{1}{2} v^\ell v^\ell + C T_\ell\right)\right] = 0 \tag{12}$$

$$\frac{\partial T_\ell}{\partial t} + \frac{v^\ell \partial T_\ell}{\partial x} = 0 \tag{13}$$

In Equations 8 - 13, g refers to the continuous gas phase and ℓ refers to the suspended dense phase. Equations 3 and 4 weight the pressure gradient by the phase volume fraction whereas Equations 10 and 11 contain the entire pressure gradient term only in the continuous gas phase.

Equation 12 is the energy equation for the mixture as a whole.

In order to obtain the characteristics of the Rudinger-Chang set, the state equation is assumed as

$$\rho_g = \rho_g(P, S_g) \tag{14}$$

where P is the pressure of the gas and S_g is the entropy of the gas. Since the dense phase is assumed to not contribute to the pressure, the gas pressure is equal to the total pressure.

Equation 12 may be rewritten by use of the continuity, momentum, and energy equations for the solids and the relations $dH_g = d(C_p T_g)$ and $dU_g = d(C_v T_g)$ as

$$\frac{\partial}{\partial t}\left[\rho_g\left(U_g + \frac{1}{2} v^g v^g\right)\right] + \frac{\partial}{\partial x}\left[\rho_g v^g\left(H_g + \frac{1}{2} v^g v^g\right)\right] = 0 \tag{15}$$

Straightforward manipulation of Equation 15 yields

$$\frac{\partial S_g}{\partial t} + v^g \frac{\partial S_g}{\partial x} = 0 \tag{16}$$

Equations 13 and 16 show that T_ℓ and S_g are convected at velocities v^ℓ and v^g, respectively. Hence, T_ℓ and S_g are invariants along the two characteristic velocities $\lambda_1 = -v^\ell$ and $\lambda_2 = -v^g$. Hence only Equations 8 - 11 remain to be classified together with the equation of state, Equation 14.

Equation 8 (gas continuity) may be rewritten, using Equation 14, as

$$C_g^{-2}\left(\frac{\partial P}{\partial t} + v^g \frac{\partial P}{\partial x}\right) + \rho_g \frac{\partial v^g}{\partial x} = 0 \tag{17a}$$

where

$$C_g^{-2} \cdot \left(\frac{\partial \rho_g}{\partial P}\right)_{S_g} \tag{17b}$$

Equations 9 - 11 and 17a may be written in matrix form as

$$A \frac{\partial \vec{w}}{\partial t} + B \frac{\partial \vec{w}}{\partial x} = 0 \tag{18a}$$

where

$$\vec{w}^T = (P, \rho^{\ell}, v^g, v^{\ell}) \tag{18b}$$

$$A = \begin{bmatrix} C_g^{-2} & 0 & 0 & 0 \\ 0 & 1 & 0 & 0 \\ 0 & 0 & \rho_g & 0 \\ 0 & 0 & 0 & \rho^{\ell} \end{bmatrix} \tag{18c}$$

and

$$B = \begin{bmatrix} C_g^{-2} v^g & 0 & \rho_g & 0 \\ 0 & v^{\ell} & 0 & \rho^{\ell} \\ 1 & 0 & \rho_g v^g & 0 \\ 0 & 0 & 0 & \rho^{\ell} v^{\ell} \end{bmatrix} \tag{18d}$$

The characteristics are obtained by solving the eigenvalue problem

$$\det(A\lambda + B) \tag{19}$$

They are given by Equations 5a and 5b. The significance of the triple *degeneracy* was discussed by Sauerwein and Fendell.[11]

3. Generalization of the Rudinger-Chang UVUT Equation Set

As it stands, the Rudinger-Chang UVUT equation set is only good for suspended particle volume fractions approaching zero. A set which could be used for all volume fractions from zero to one is desirable. If the entire pressure drop is assumed to take place in the vapor phase, a logical generalization of the Rudinger-Chang UVUT equation set to gas-liquid systems is

Continuity

$$\frac{\partial(\alpha^g \rho_g)}{\partial t} + \frac{\partial}{\partial x}(\alpha^g \rho_g v^g) = 0 \tag{20}$$

$$\frac{\partial(\alpha^\ell \rho_\ell)}{\partial t} + \frac{\partial}{\partial x}(\alpha^\ell \rho_\ell v^\ell) = 0 \tag{21}$$

Momentum

$$\frac{\partial(\alpha^g \rho_g v^g)}{\partial t} + \frac{\partial}{\partial x}(\alpha^g \rho_g v^g v^g) + \frac{\partial P}{\partial x} = 0 \tag{22}$$

$$\frac{\partial(\alpha^\ell \rho_\ell v^\ell)}{\partial t} + \frac{\partial}{\partial x}(\alpha^\ell \rho_\ell v^\ell v^\ell) = 0 \tag{23}$$

Energy

$$\frac{\partial S_g}{\partial t} + v^g \frac{\partial S_g}{\partial t} = 0 \tag{24}$$

$$\frac{\partial S_\ell}{\partial t} + v^\ell \frac{\partial S_\ell}{\partial t} = 0 \tag{25}$$

4. Characteristics Analysis for the Generalized Rudinger-Chang UVUT Equation Set

Equations 24 and 25 show that S_g and S_ℓ propagate along v^g and v^ℓ. Hence, S_g and S_ℓ are invariants along the characteristic velocities

$\lambda_1 = -v^g$ and $\lambda_2 = -v^\ell$.

The state equations

$$\rho_\ell = \rho_\ell(P, S_\ell) \tag{26a}$$

and

$$\rho_g = \rho_g(P, S_g) \tag{26b}$$

complete the set.

Alternative energy equations could have been written which propagate the phase energies along with the phase velocities. The state equations and single phase sound speeds would be changed accordingly. The form of the energy equations is not the central issue in this paper. Equations 20 - 23 are adequate for characteristics analysis.

Equations 20 - 23 may be written in the matrix form of Equations 18a with

$$\vec{w}^T = (\alpha^g, P, v^g, v^\ell) \tag{27a}$$

$$A = \begin{bmatrix} \rho_g & \alpha^g c_g^{-2} & 0 & 0 \\ -\rho_\ell & \alpha^\ell c_\ell^{-2} & 0 & 0 \\ 0 & 0 & \alpha^g \rho_g & 0 \\ 0 & 0 & 0 & \alpha^\ell \rho_\ell \end{bmatrix} \tag{27b}$$

and

$$B = \begin{bmatrix} \rho_g v^g & \alpha^g C_g^{-2} v^g & \alpha^g \rho_g & 0 \\ -\rho_\ell v^\ell & \alpha^\ell C_\ell^{-2} v^\ell & 0 & \alpha^\ell \rho_\ell \\ 0 & 1 & \alpha^g \rho_g v^g & 0 \\ 0 & 0 & 0 & \alpha^\ell \rho_\ell v^\ell \end{bmatrix} \tag{27c}$$

where

$$C_g^{-2} = \left(\frac{\partial \rho_g}{\partial P}\right)_{U_g \text{ or } S_g} \tag{28a}$$

and

$$C_\ell^{-2} = \left(\frac{\partial \rho_\ell}{\partial P}\right)_{U_\ell \text{ or } S_\ell} \tag{28b}$$

The characteristics are obtained from the eigenvalue problem, Equation 19. They are all real and are given by

$$\lambda_3 = -v^\ell \tag{29a}$$

$$\lambda_4 = -v^\ell \tag{29b}$$

and

$$\lambda_{5,6} = -v^g \pm \sqrt{\frac{\rho_m C_m^2}{\rho_g}} \tag{29c}$$

where C_m is the so-called homogeneous or "frozen" sound speed given by[1]

$$C_m = [\rho_m(\alpha^\ell C_\ell^{-2} \rho_\ell^{-1} + \alpha^g C_g^{-2} \rho_g^{-1})]^{-1/2} \tag{30}$$

and ρ_m is the average density given by

$$\rho_m = \alpha^g \rho_g + \alpha^\ell \rho_\ell \tag{31}$$

The characteristics for the Rudinger-Chang set are obtained when $\alpha^{\ell} = 0$ in Equation 29c. If the liquid is assumed to be the continuous phase, the subscripts and superscripts ℓ and g are merely interchanged in the preceding analysis. The generalization of $\lambda_{5,6}$ is, therefore,

$$\lambda_{5,6} = -v^{c} \pm C_m \left(\rho_m/\rho_c\right)^{\frac{1}{2}} \tag{32}$$

where c denotes the continuous phase.

5. Numerical Computations and Comparison with Experiment

Both equation sets, Equations 1 - 4 and 20 - 23 were programmed for constant phase energies using an implicit numerical scheme being developed at Aerojet Nuclear Company which is based on the modified ICE technique developed by Los Alamos Scientific Laboratory[12]. The solution sequence is outlined in the Appendix.

In order to calibrate the pressure propagation rates obtained from the UVUT computer code, the following hypothetical blowdown was run with a steam-water nonequilibrium mixture. A uniform fifty-volume-percent steam-water mixture is initially quiescent in a long closed horizontal pipe. The pressure is uniform at 1000 psia and the temperatures of the phases are approximately 1400°F steam and 100°F water. All heat transfer and friction are suppressed for these computer runs. At $t=0^{+}$, one end of the pipe is opened to a 900 psia reservoir. The pressure response at the closed end is shown in Figure 1. The curve marked UVUT is the result computed using Equations 1 - 4 and the curve marked EVET is the result computed for a 1400°F superheated steam blowdown. The pressure minimum results when the 100 psi decompression wave reflects a wave of like kind. Hence the pressure falls to nearly 800 psia which is 100 psia below the ambient pressure. As can be seen in the figure, the pressure propagation rate in the two phase mixture obtained using Equations 1 - 4 is nearly identical to that for steam alone and indicates that the pressure wave travelled at the stratified sound speed which is nearly equal to the steam sound speed over most of the volume fraction range. Although not shown, the pressure response for the blowdown of subcooled 100°F water alone was considerably different.

Two computer runs were made with the modified Rudinger-Chang equation set, Equations 20 - 23, one with the pressure dron in the vapor phase and one with the pressure drop in the liquid phase. The same initial and boundary conditions for the two-phase fifty-volume-percent steam-water mixture were used as shown in Figure 1. Pressure response profiles for these two runs are shown in Figure 2 along with the results computed from Equations 1 - 4. Slight pressure undershoots below 900 psia are purely numerical. As can be seen, the pressure propagation behavior is entirely different for the different equation sets. In order to determine whether the computed trends were correct, the following calculations were made.

At 1000 psia, the sound speeds of the two phases are 2517 ft/sec (vapor) and 5048 ft/sec (liquid). The phase densities are 0.917 lb_m/cu ft. (vapor) and 62.18 lb_m/cu ft (liquid). The stratified sound speed, C_s, is computed to be 2531 ft/sec and the sound speeds for the modified Rudinger-Chang equation set are

$$\frac{\partial P}{\partial x}_{\text{liquid}} : 431.5 \text{ ft/sec}$$

$$\frac{\partial P}{\partial x}_{\text{vapor}} : 3553.4 \text{ ft/sec}$$

These numbers corroborate the observations that

(1.) The propagation rate of the pressure pulse through the two phase mixture calculated from Equations 1 - 4 is practically identical to that through pure steam. C_s is slightly higher, so the pressure falls slightly sooner at the closed end as shown in Figure 1.

(2.) The propagation rate of the pressure pulse calculated from the modified Rudinger-Chang equation set with the pressure gradient in the liquid phase considerably lags the results from Equations 1 - 4 as shown in Figure 2. If the pressure gradient is in the vapor phase, the propagation rate is highest. As shown in Figure 2, the pressure profile for 2 msec practically coincides with the results from Equations 1 - 4, for 3 msec.

Propagation rates are difficult to deduce from the numerical computations because of the presence of numerical diffusion. If the standard is taken to be the single phase pressure propagation rate of superheated steam, the amount of numerical smearing can be estimated in the following manner. For the sound speed of superheated steam (2517 ft/sec) and the pipe length (13.44 ft), computations show that the pressure should not begin to fall below 1000 psia at the closed end until 5.34 msec. At 5.34 msec however, the computed pressure has already fallen to approximately 939 psia as shown in Figure 1. This discrepancy of 61 psia is about 32 percent of the difference between the initial (1000 psia) and the minimum (810 psia) pressure at the closed end for the Δt and Δx used. Use of this percent pressure change as a numerical smearing criterion yields a propagation rate for Equations 1 - 4 of 2575 ft/sec which is somewhat greater than the predicted stratified sound speed of 2531 ft/sec. The propagation rate for the modified Rudinger-Chang equation set with the pressure gradient in the vapor was estimated to be 3630 ft/sec. Use of the pressure profiles from Figure 2 yield the values shown in Table 1. Propagation results vary because the phases are accelerating. Calculation of the propagation rates from response times at the closed end when available are probably more accurate because the phase velocities are exactly zero there. For longer times, the propagation rates obtained from Figure 2 tend to agree more closely with the closed end result because the distance at which the pressure has fallen 32 percent is becoming closer to the closed end. The case of the pressure gradient in the liquid phase was not computed for long enough time for the pressure to begin falling at the closed end because the computer time would be excessive at the uniform (0.1 msec) size time step used. The propagation rate for this case was estimated from Figure 2 and the results are also given in Table 1. All the pressure propagation rates are on the same order of magnitude as those predicted from the characteristics analysis.

The experiment chosen for comparison of computed pressure pulse propagation rates is that of Reference 3. A schematic of the apparatus is reproduced in Figure 3. Air is bubbled into the bottom of a vertical pipe filled with water. The void fraction is measured by a gamma ray attenuation device. At the beginning of the run, a diaphragm is ruptured and a step decrease or increase in pressure occurs at the top of the vertical pipe. The pressure transient is measured at three stations. From

these measurements, the propagation rate was deduced from delay times of the pressure wave front. The results for the runs are reproduced in Figure 4. Also plotted by the authors is the "frozen" two phase sound speed and the equilibrium two phase sound speed. An apparent jump occurs in the pressure wave velocity data at 50 percent void fraction. This jump will be discussed in more detail later as will the additional curves.

The experiment was modelled numerically in the following manner. Initially the pressure is assumed uniform at 1.75 bar (35.38 psia) and the void fraction is uniform at the initial value as measured in the experiment. Since the air supply was not given, an average initial bubble rise velocity of 2 ft/sec was assumed as reasonable for the air. The temperature was assumed to be constant at 70°F. Further assumptions are incompressible liquid and an isothermal ideal gas approximation for the air. At $t = 0^+$, the pressure is changed at the top (2.08m, or 6.824 ft) to ambient pressure. At the bottom (zero height), the air velocity is maintained to be 2 ft/sec during the run. No friction or heat and mass transfer were used.

Pressure response profiles computed from Equations 1 - 4 and the modified Rudinger-Chang equation set with the pressure gradient in the liquid phase are plotted in Figure 5. The conditions for this run were an initial volume fraction of air equal to 30 percent and a depressurization from 1.75 bar (25.38 psia) to 1.0 bar (14.50 psia). The general shape of the pressure profiles is quite similar to that for the horizontal pipe blowdown as shown in Figure 2. The amount of numerical undershoot is much less evident. The trend is the same, with the propagation rates computed from the modified Rudinger-Chang equation set lagging considerably behind those computed from Equations 1 - 4. At an air volume fraction of 30 percent the stratified sound speed calculated from Equation 6 using an isothermal air sound speed of 956 ft/sec and an infinite liquid sound speed is 958.3 ft/sec. The sound speed calculated from Equation 32 with zero velocity and liquid being the continuous phase is 80 ft/sec. The values of the propagation rate deduced from

the pressure profile response, and the closed end response from Figure 6 are summarized in Table 2. The trends are the same as in Table 1. The very high value of the propagation rate at 1 msec for the Rudinger-Chang equation set with the pressure gradient in the liquid phase is probably caused by the relatively coarse nodalizing. The most important observation is that the propagation rate is definitely on the order of the sound speeds calculated from the characteristics analysis. Although the time scale is different, Figure 6 does show pressure undershoots at the middle and bottom of the horizontal test section similar to those exhibited by the experimental data.[3]

Another computer calculation for the modified Rudinger-Chang equation set at 10 percent vapor was performed in order to predict the trend that the propagation rate should increase as the volume fraction decreases (Table 2)

Since the computer runs demonstrated that pressure pulses travel at essentially the sound speeds obtained from characteristics analysis, these expressions themselves may now be used to further analyze the capability of the equation sets under consideration to model the experiment. Clearly Equations 1 - 4 predict propagation rates which are much too high. The propagation rates predicted by the modified Rudinger-Chang equation set with the pressure gradient in the liquid are summarized in Table 3 and plotted in Figure 4. Curve 4 is Equation 32 with an isothermal air sound speed of 956 ft/sec. Curve 3 is Equation 32 with an adiabatic air sound speed of 1128 ft/sec. As α_g goes to zero, Curve 3 merges with the "frozen" adiabatic sound speed, Curve 1, whereas for larger volume fractions Curve 3 falls below Curve 1. Curve 4 merges with the equilibrium sound speed, Curve 2. If the vapor is taken to be the continuous phase, the propagation rate is far too high as shown in Table 3. If the continuous phase is assumed to become the vapor at 50 volume percent voids, the apparent jump in the propagation rate is explained. However, the propagation rate is significantly higher than the data. The jump is from 61.5 ft/sec to 957 ft/sec using isothermal gas sound speeds. The sound speeds obtained from charac-

teristics analysis which are summarized in Table 3 are plotted in Figure 7, where the approximate range of data is indicated. For larger α^g, the highest curve, Curve 1, begins to agree with a model for idealized slug flow[13].

6. Conclusions

Several published two phase flow equation sets have been studied numerically. Pressure pulses were found to propagate at speeds essentially equal to the sound speeds obtainable from characteristics analysis. Comparisons of these sound speeds with experimental data show that the modified Rudinger-Chang equation set exhibits propagation behavior more nearly in agreement with the data. At low volume fraction, the results from the modified Rudinger-Chang set reduce to the homogeneous or "frozen" sound speed. At intermediate volume fractions, for which a transition from bubbly to slug flow is observed to occur experimentally, no equation set adequately predicts the experimental propagation rates. Retention of regime dependent transient flow forces such as used by Mecredy and Hamilton[14] may rectify the situation. The existence of an apparent jump in the data at a volume fraction of 50 percent can be explained by the modified Rudinger-Chang equation set, however, the magnitude is greater than the experimental value.

7. References

1. Wallis, G. B., One-Dimensional Two-Phase Flow , McGraw-Hill, New York (1969).

2. Rudinger, George and Chang, Angela, "Analysis of Nonsteady Two-Phase Flow", Physics of Fluids, 7, pp 1747 - 1754, 1964.

3. Miyazaki, Keiji, Fujii-e, Yoichi, and Suita, Tokuo, "Propagation of Pressure Wave in Air-Water Two-Phase System, (I)", J. Nuclear Science and Technology, 8, 606 - 613, November 1971.

4. Hsu, Y. Y. Review of Critical Flow Rate, Propagation of Pressure Pulse and Sonic Velocity in Two-Phase Flow , NASA Technical Note NASA TND-6814, Washington, (June 1972).

5. Gidaspow, Dimitri, "Introduction to 'Modeling of Two Phase Flow'", Round Table Discussion (RT-1-2). To appear in Vol. VII of the Proceedings of the 5th International Heat Transfer Conference, Tokyo, September 3-7, 1974.

6. Gidaspow, Dimitri, Lyczkowski, R. W., Solbrig, C. W., Hughes, E. D. and Mortensen, G. A., "Characteristics of Unsteady One-Dimensional Two-Phase Flow", Trans. Am. Nucl. Soc., 17, 249 (1973).

7. Giot, M. and Fritte, A., "Two-Phase Two- and One- Component Critical Flows With the Variable Slip Model" pp 651 - 670 Progress in Heat and Mass Transfer, Vol. 6, Proceedings of the International Symposium on Two-Phase Systems, Haifa, 1971, G. Hetsroni, S. Sideman and J. P. Hartnett, Editors, Pergamon Press, Oxford (1972).

8. Delhaye, J. M., Equations generales des encoulments diphasiques, lere partie: Equations generales de conservation, CEA-R-3429(I) 2 eme partie: Complements et remarques, CEA-R-3429(2). CENG (1968).

9. Vernier, Ph., and Delhaye, J. M., "Equations generales des ecoulments diphasiques appliquees a la thermohydrodynamique des reacteurs nucleaires a eau bouillante", EPE, 4, no. 1 - 2, pp 5 - 46 1968.

10. Boure, J., Dynamiques des ecoulments diphasiques: Propagation de Petites Perturbations, CEA-R-4456, CENG (1973).

11. Sauerwein, H., and Fendell, F. E., "Method of Characteristics in Two-Phase Flow" Phys. Fluids, 8, 1564 - 1565, 1965.

12. Harlow, F. H. and Hirt, C. W., "A Numerical Fluid Dynamics Calculation Method for All Flow Speeds", J. Comp. Physics, 8, 197 - 213, 1971.

13. Henry, R. E., Grolmes, M. A., and Fauske, H. K. "Propagation Velocity in Gas-Liquid Mixtures", Co-Current Gas-Liquid Flows., E. Rhodes and D. S. Scott, Editors, Plenum Press, New York (1960).

14. Mecredy, R. C. and Hamilton, L. J., "The Effects of Nonequilibrium Heat, Mass and Momentum Transfer on Two-Phase Sound Speed", Int. J. Heat Mass Transfer, 15, pp 61 - 72, 1972.

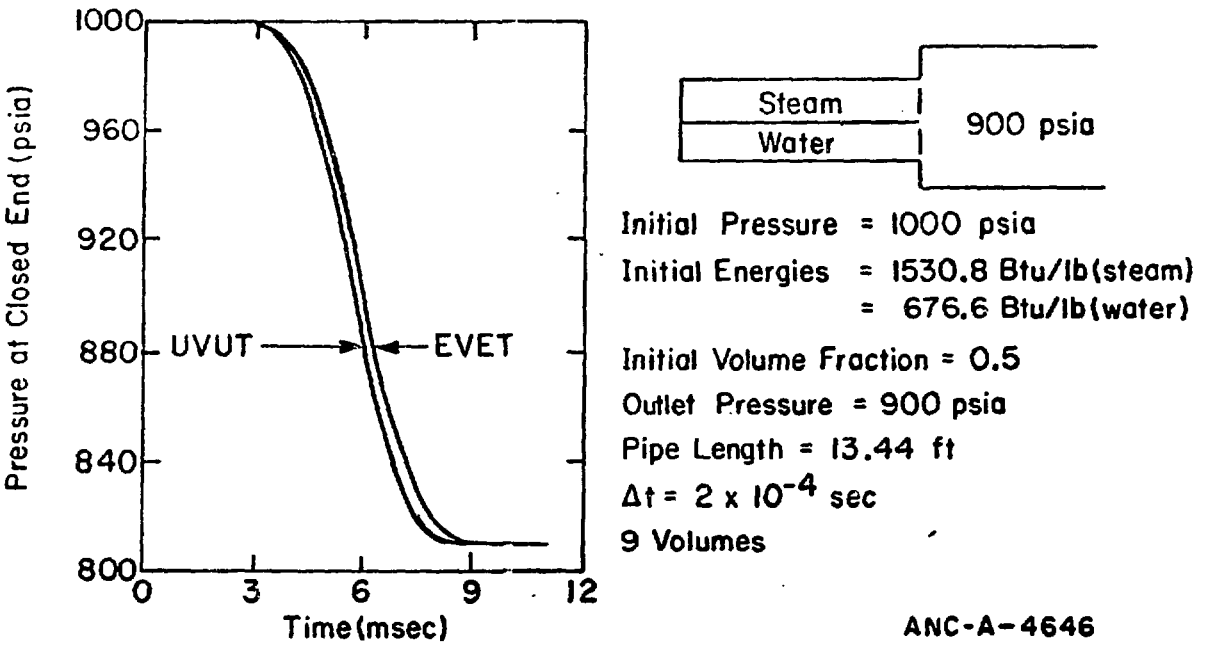

Figure 1. Pressure Response at the Closed End of a Horizontal Pipe during Blowdown for a Two-Phase Mixture using Equations 1-4 and for Single-Phase Superheated Steam.

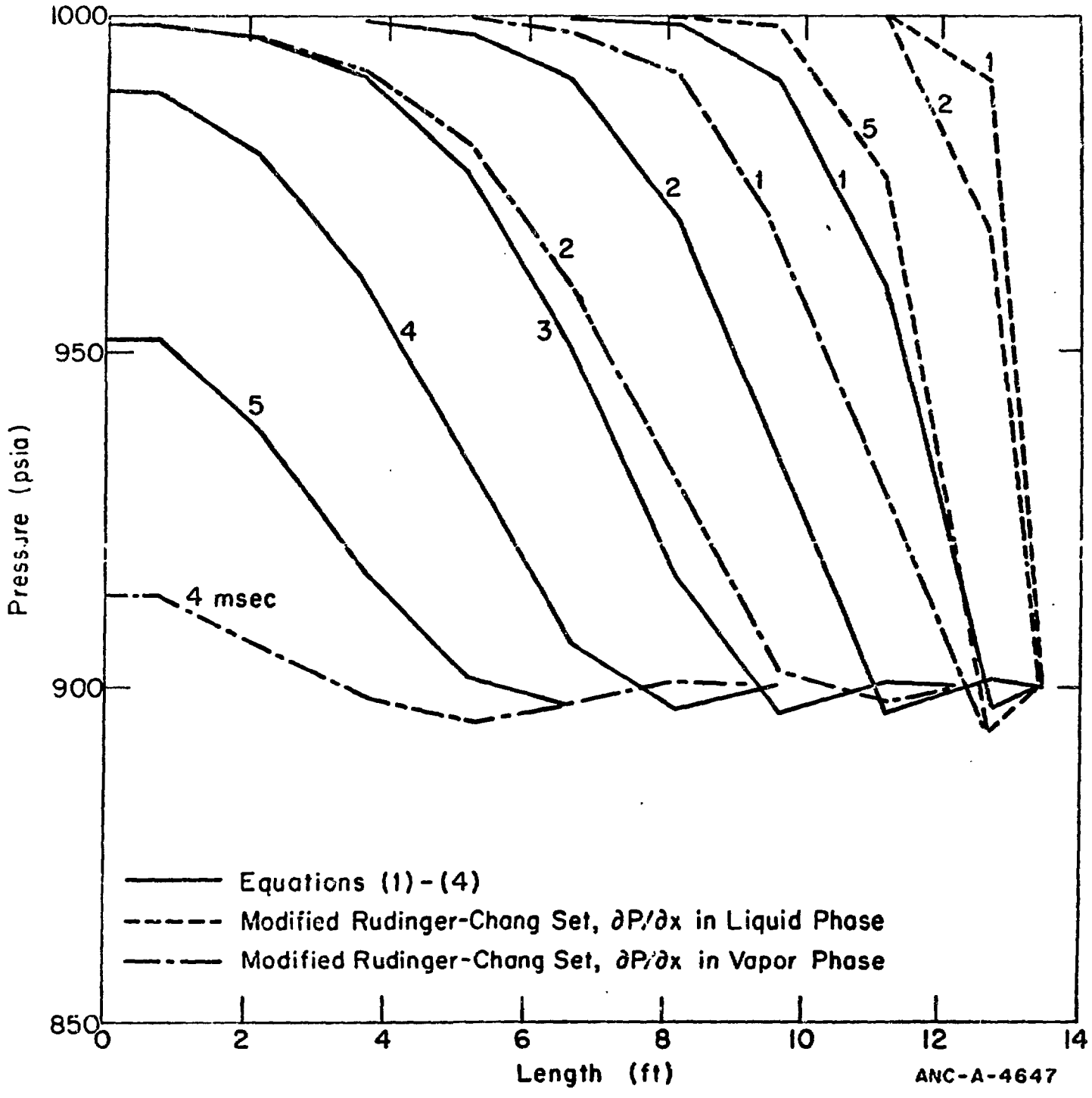

Figure 2. Pressure Response Profiles Obtained from Three Two-Phase Models for a Horizontal Pipe during Blowdown for a Two-Phase Mixture.

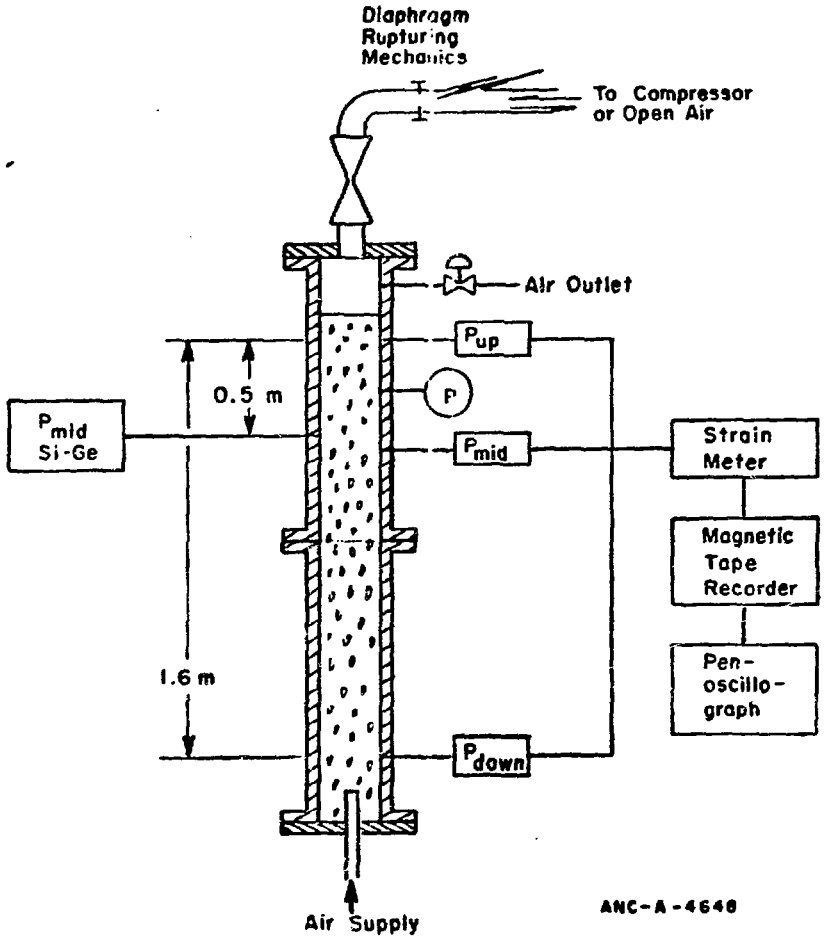

Figure 3. Schematic diagram of Experimental Setup[3]

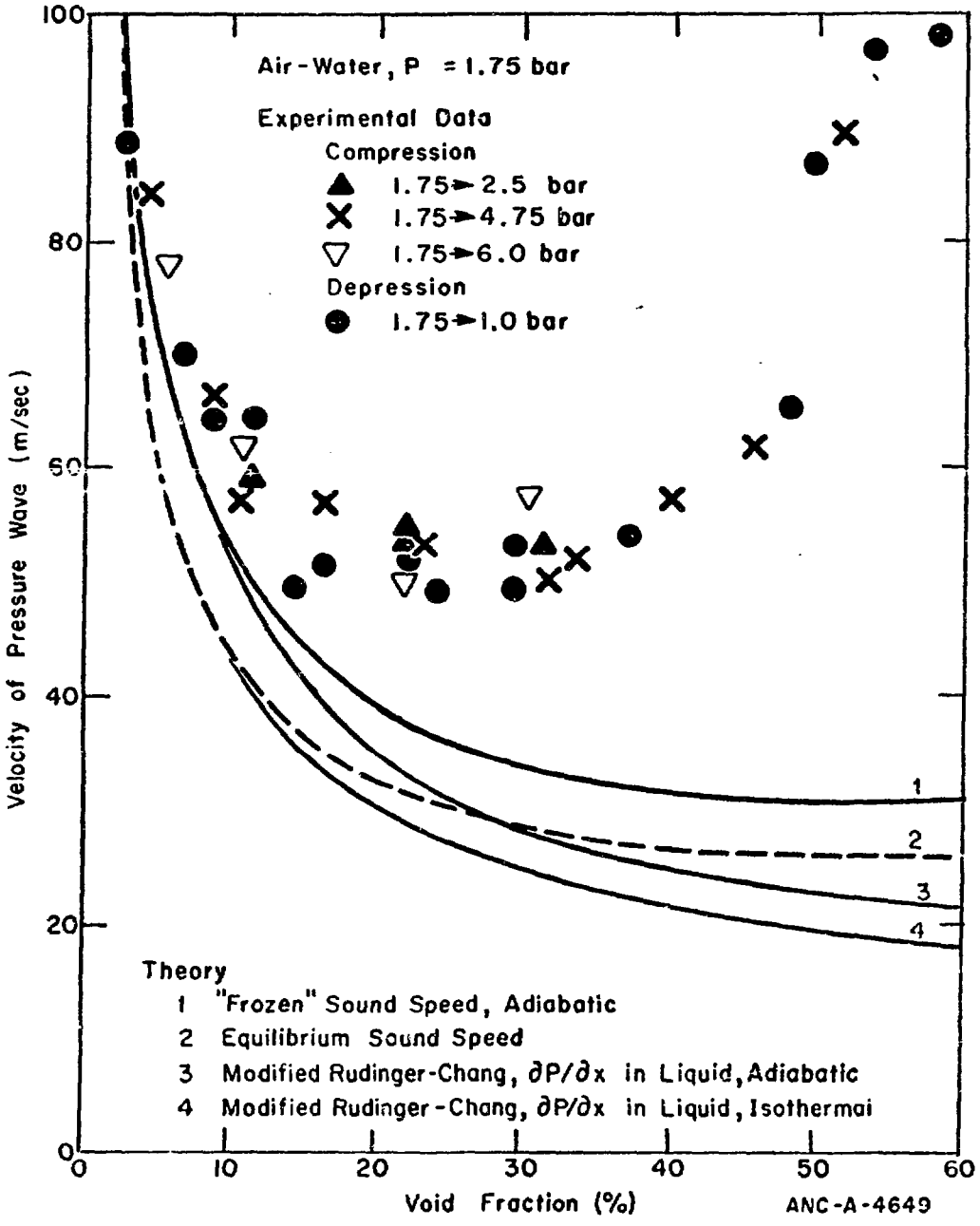

Figure 4. Front Velocity vs. Void Fraction Curves for Initial Pressure of 1.75 Bar[3].

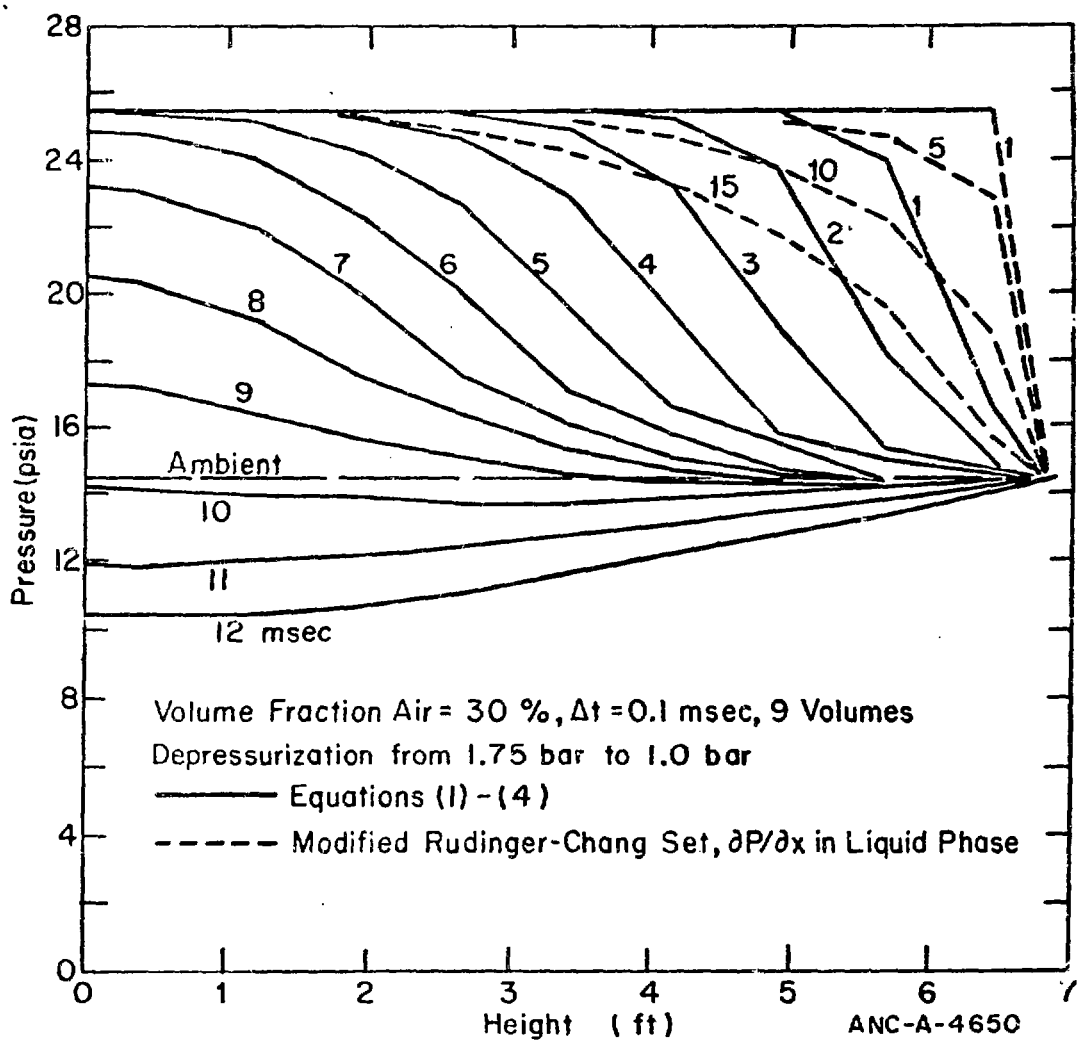

Figure 5. Pressure Profiles for the Miyazaki et al[3] experiment

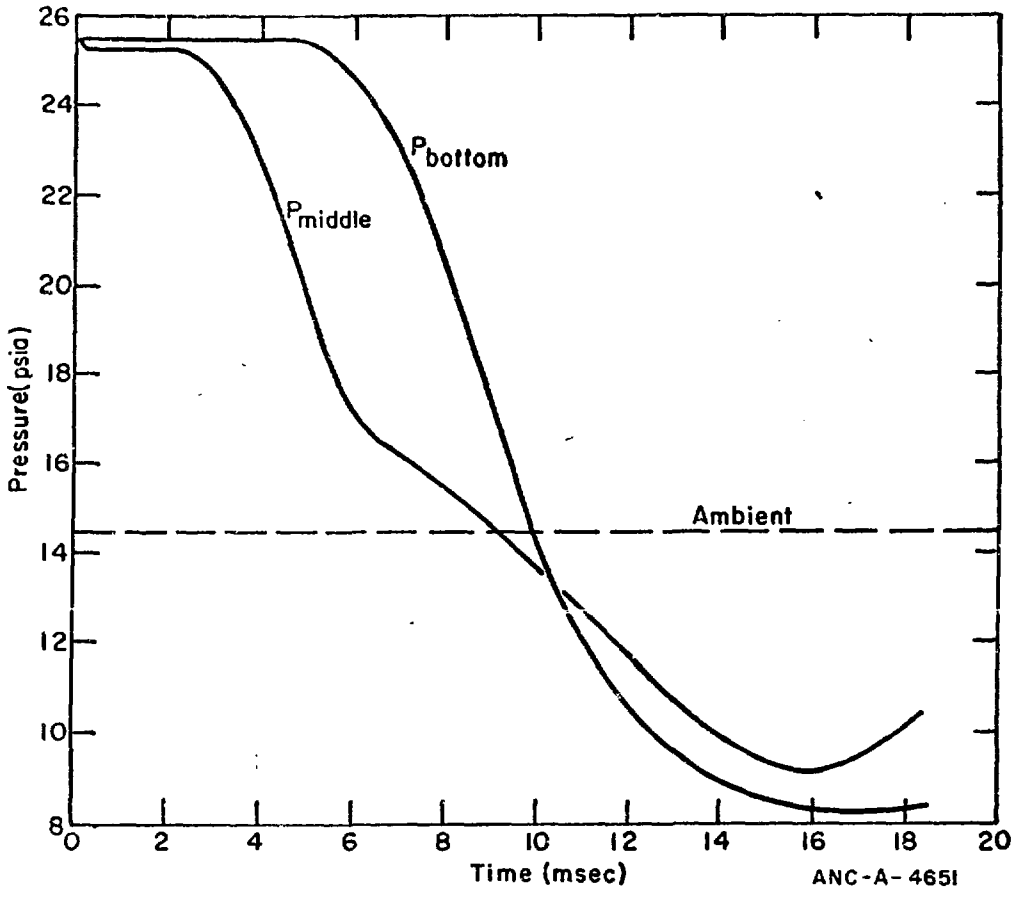

Figure 6. Pressure Response at Two Station for the Miyazaki et al[3] Experiment using Equations 1 - 4. Volume Fraction = 30 Percent

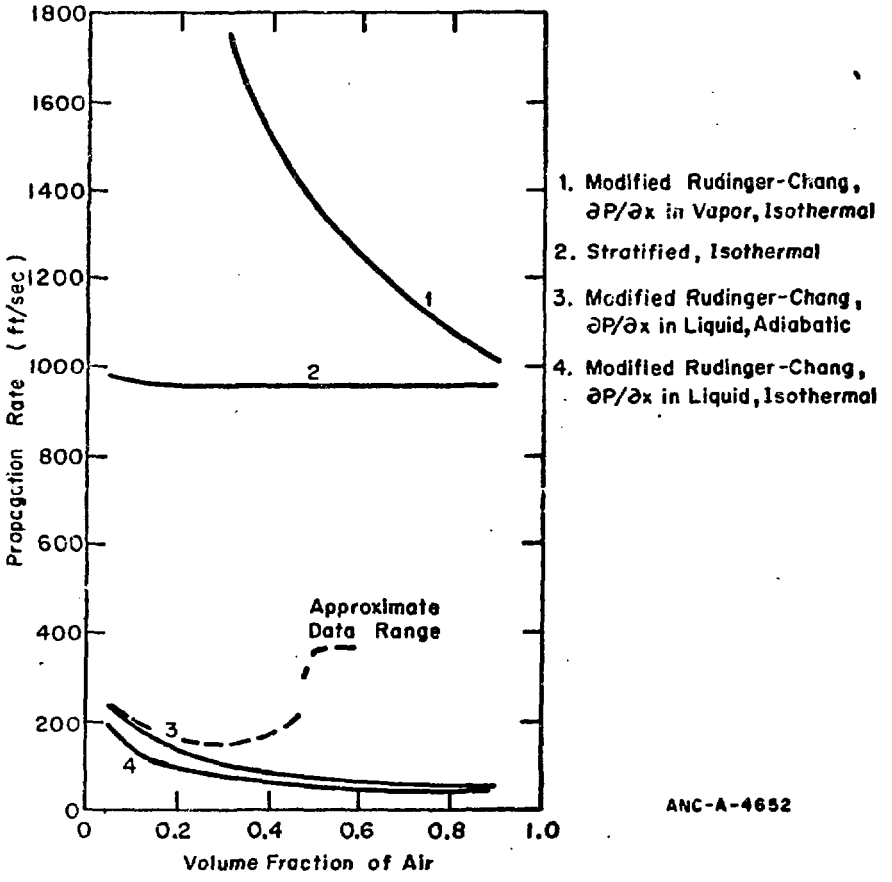

Figure 7. Comparison of Two-Phase Sound Speeds Computed from Characteristics Analysis - Air-Water System at 1.75 Bar.

Table 1

Propagation Rates For Horizontal Pipe;

50 Percent Water-Steam Mixture at 1000 psia in ft/sec

(Deduced from Figures 1 and 2)

Time (msec)	Equations 1 - 4 (Theory = 2531)	Modified Rudinger-Chang Set	
		∂P/∂x in Liquid (Theory = 432)	∂P/∂x in Vapor (Theory = 3553)
1	2690	540	3840
2	2595	370	3670
4	2585	---	----
5	----	430	----
Closed end result	2575	---	3630

Table 2

Propagation Rates For the Miyazaki et al Experiment[3]

in ft/Sec(Deduced from Figures 5 and 6)

Time (msec)	30 Percent Air - Water Mixture		10 Percent Air-Water Mixture
	Equations 1 - 4 (Theory = 959)	Modified Rudinger - Chang set, ∂P/∂x in Liquid (Theory = 80)	Modified Rudinger - Chang Set, ∂P/∂x in Liquid (Theory = 137)
1	950	270	244
2	840	---	---
5	800	70	124
10	---	110	330
15	---	135	285
Closed end result	920	---	---

Table 3

Comparison of Two-Phase Sound Speeds Computed from Characteristics Analysis for Air-Water Mixture at 1.75 Bar. Incompressible Water, ρ_g = 0.129 lbm/ cu ft., ρ_ℓ = 62.43 lb_m/ cu ft., Isothermal Air Sound Speed = 956 ft/sec, Adiabatic Air Sound Speed = 1131 ft/sec.

Volume fraction air	Modified Rudinger - Chang Set			Equations 1 - 4 Isothermal
	$\partial P/\partial x$ in Liquid		$\partial P/\partial x$ in Vapor	
	Isothermal	Adiabiatic	Isothermal	
0.05	194	229	----	974
0.10	137	192	3023	964
0.20	97	115	2137	960
0.30	79	94	1745	958
0.40	69	81	1511	957
0.50	62	73	1352	957
0.60	56	66	1234	956
0.70	52	61	1142	956
0.80	49	58	1068	956
0.90	46	54	1007	956

APPENDIX. Outline of Numerical Solution Procedure For UVUT Code